

Baryon topology in hypersphere soliton model

Soon-Tae Hong*

Center for Quantum Spacetime and Department of Physics, Sogang University, Seoul 04107, Korea

(Dated: February 20, 2022)

Exploiting a topological soliton on a hypersphere, we construct baryon charge profile functions by calculating explicit isoscalar and isovector electric charge densities. In this approach we depict the charge density profiles for proton and neutron plotted versus hypersphere third angle μ . We next investigate the topologies of the hypersphere soliton via the Möbius strips which are related with the tubular neighborhoods of the half-twist circles inside the manifold S^3 . In particular, we show that in the hypersphere soliton the baryons are delineated in terms of the knot structure of the Möbius strips. We find that the knot structure of the Möbius strip type half-twist circles inside the nucleons can explain the gluon effect and confinement problem of the quark related model such as QCD.

Keywords: hypersphere soliton, baryon, charge density profiles, knot, twist circle

I. INTRODUCTION

It is well known that the Dirac Hamiltonian scheme has been employed [1–4], to convert the second class constraints into the first class ones. Moreover, making use of the Dirac quantization, there have been many attempts for quantizing the constrained systems, in order to obtain rigorous energy spectrum and investigate BRST [5–7] symmetries involved in the systems. In particular, the first order tetrad gravity has been investigated in the Dirac Hamiltonian scheme to see that the second class constraints reduce the theory to second order tetrad gravity and the first class constraints are different from those in the second order formalism, but satisfy the same gauge algebra if one uses Dirac brackets [2]. There have been attempts to study the quantum BRST charge for quadratically nonlinear Lie algebras, and to derive a condition which is necessary and sufficient for the existence of a nilpotent BRST charge [3]. In a (1+1) dimensional supersymmetric soliton, topological boundary conditions and the BPS bound have also been investigated to fix ambiguities in the quantum mass of the soliton [8]. Moreover the constrained Hamiltonian quantization has been applied to the cosmological perturbation theory [9, 10].

On the other hand, it is well known that the standard Skyrmin model [4, 11–13] is a constrained Hamiltonian system. In particular, this Skyrmin has been analyzed via the canonical quantization in the second class formalism, to study the baryon kinematics and its static properties [12]. Later, the hypersphere soliton model (HSM) has been proposed on the curved manifold [14] to obtain a topological lower bound on the baryon soliton energy and a set of equations of motion. Next we have newly predicted the baryon physical properties, such as masses, charge radii and magnetic moments in the HSM [13].

Recently we have studied a mechanism of baryon mass genesis by exploiting a pulsating soliton in HSM [15]. To do this, first we have exploited the first class Hamiltonian to quantize the hypersphere soliton, and then have predicted the axial coupling constant whose value is in good agreement with its corresponding experimental data. Next we have formulated the intrinsic frequencies of the pulsating baryons. Explicitly, we have evaluated the intrinsic frequencies ω_N and ω_Δ of the nucleon and delta hyperon, respectively, to obtain the identity $\omega_\Delta = 2\omega_N$.

In this paper we will consider the HSM, to study profile functions inside baryons. Furthermore, in the HSM, we will probe theoretically the baryon topology to investigate their charge density profiles and knot structure of Möbius strips associated with the tubular neighborhoods of the half-twist circles inside the topological soliton.

In Sec. II, we will briefly construct baryon formalism to study the profile function. In Sec. III, we will analyze the charge profile functions of nucleons. In Sec. IV, we will investigate the knot structures of the Möbius strip type half-twist circles inside the nucleons. Sec. V includes conclusions. In Appendix A, hypersphere geometry is summarized, and the Hopf fibration [16–18] is discussed on the hypersphere.

*Electronic address: galaxy.mass@gmail.com

II. BARYON CHARACTERISTICS IN HSM

In this section, in the HSM [13–15] we briefly investigate the profile function in Fig. 1(a) in the identity map associated with the BPS bound in the baryon soliton energy. To do this, we start with the Skyrme Lagrangian density

$$\mathcal{L} = \frac{f_\pi^2}{4} \text{tr}(\partial_\mu U^\dagger \partial^\mu U) + \frac{1}{32e^2} \text{tr}[U^\dagger \partial_\mu U, U^\dagger \partial_\nu U]^2, \quad (2.1)$$

where U is an $SU(2)$ chiral field, and f_π and e are a pion decay constant and a dimensionless Skyrme parameter, respectively. Next the quartic term is necessary to stabilize the soliton in the baryon sector. Now we proceed to investigate baryon phenomenology by using the hyperspherical metric derived in Appendix A

$$ds^2 = \lambda^2 d\mu^2 + \lambda^2 \sin^2 \mu (d\theta^2 + \sin^2 \theta d\phi^2). \quad (2.2)$$

Here the ranges of the hyperspherical coordinates are given by $0 \leq \mu \leq \pi$, $0 \leq \theta \leq \pi$ and $0 \leq \phi \leq 2\pi$, and λ ($0 \leq \lambda < \infty$) is the radius parameter of the hypersphere S^3 . Note that S^3 is described in terms of the three dimensional hypersphere coordinates (μ, θ, ϕ) and the radius parameter λ .

In the hypersphere soliton on S^3 , we obtain the soliton energy

$$E = \frac{f_\pi}{e} \left[2\pi L \int_0^\pi d\mu \sin^2 \mu \left(\left(\frac{df}{d\mu} + \frac{1}{L} \frac{\sin^2 f}{\sin^2 \mu} \right)^2 + 2 \left(\frac{1}{L} \frac{df}{d\mu} + 1 \right)^2 \frac{\sin^2 f}{\sin^2 \mu} \right) + 6\pi^2 \right], \quad (2.3)$$

where $L = ef_\pi \lambda$ ($0 \leq L < \infty$) is a radius parameter expressed in dimensionless units. Here $f(\mu)$ is the profile function for the hypersphere soliton, and satisfies $f(0) = \pi$ and $f(\pi) = 0$ for unit baryon number. The above soliton energy has the BPS bound in the soliton model [13–15, 18, 19] to yield the inequality

$$E \geq \frac{6\pi^2 f_\pi}{e} |B|, \quad (2.4)$$

where B is given by [13]

$$B = -\frac{2}{\pi} \int_0^\pi d\mu \sin^2 \mu \frac{df}{d\mu}. \quad (2.5)$$

Note that B is a conserved topological charge which is a baryon number in the HSM. For a single soliton, the topological charge is one [13–15, 18, 19]. In the cases of multi-Skyrmion solutions with $|B| > 1$, the soliton energies will not satisfy the bound in Eq. (2.4) and possess much higher energy. The hedgehog solutions for the multi-Skyrmions then have been shown to be almost certainly all unstable saddle-points of the energy [18].

The profile function f in the soliton energy lower bound satisfies equations of motion,

$$\frac{df}{d\mu} + \frac{1}{L} \frac{\sin^2 f}{\sin^2 \mu} = 0, \quad \frac{1}{L} \frac{df}{d\mu} + 1 = 0. \quad (2.6)$$

One of the simplest solutions of (2.6) is the identity map

$$f(\mu) = \pi - \mu \quad (2.7)$$

with the condition $L = L_B$, where $L_B \equiv ef_\pi \lambda_B = 1$. The profile function $f(\mu)$ in the identity map, associated with the BPS bound in the soliton energy, is depicted in terms of the angle μ in Fig. 1(a). The fixed value $L = L_B$ can be used to obtain the soliton energy lower bound

$$E = \frac{6\pi^2 f_\pi}{e}. \quad (2.8)$$

From now on we will use the condition $L_B = 1$ to predict the physical quantities such as moment of inertia, baryon masses and charge radii in the HSM.

After performing the Dirac quantization in the first class formalism [1, 4], we obtain the modified Hamiltonian spectrum [4, 15]

$$\langle H \rangle = E + \frac{1}{2I} \left[I(I+1) + \frac{1}{4} \right], \quad (2.9)$$

where I ($= 1/2, 3/2, \dots$) are isospin quantum numbers of baryons. Here E is given by (2.8) and \mathcal{I} is the moment of inertia

$$\mathcal{I} = \frac{3\pi^2}{e^3 f_\pi}. \quad (2.10)$$

As a result, we newly construct the Weyl ordering corrected nucleon and delta hyperon masses, respectively [15]

$$M_N = ef_\pi \left(\frac{6\pi^2}{e^2} + \frac{e^2}{6\pi^2} \right), \quad M_\Delta = ef_\pi \left(\frac{6\pi^2}{e^2} + \frac{2e^2}{3\pi^2} \right). \quad (2.11)$$

Next, in the HSM we obtain the charge radii [13, 15]

$$\langle r^2 \rangle_{M,I=0}^{1/2} = \langle r^2 \rangle_{M,I=1}^{1/2} = \langle r^2 \rangle_{M,p}^{1/2} = \langle r^2 \rangle_{M,n}^{1/2} = \langle r^2 \rangle_{E,I=1}^{1/2} = \sqrt{\frac{5}{6}} \frac{1}{ef_\pi}, \quad (2.12)$$

where the subscripts E and M stand for the electric and magnetic radii, respectively.

Making use of the charge radii in (2.12) we fix the value of $\langle r^2 \rangle_{M,p}^{1/2}$ with the corresponding experimental data $\langle r^2 \rangle_{M,p}^{1/2} = 0.80$ fm. We can then have

$$ef_\pi = 225.23 \text{ MeV} = (0.876 \text{ fm})^{-1}. \quad (2.13)$$

Note that, inserting $ef_\pi = (0.876 \text{ fm})^{-1}$ into the condition $L_B = 1$, we obtain $\lambda_B = 0.876$ fm. The hypersphere soliton is thus defined in terms of the fixed radius parameter λ_B which is comparable to the predictions for the charge radii in (2.12). In other words, in the HSM the Universe \mathcal{U} is given by a sum of two subspaces, namely $\mathcal{U} = V_B(\lambda \leq \lambda_B) \oplus \bar{V}_B(\lambda > \lambda_B)$ where $V_B(\lambda \leq \lambda_B)$ and $\bar{V}_B(\lambda > \lambda_B)$ are the volume subspaces inside and outside the hypersphere soliton, respectively. Moreover, in this model the baryons are described in terms of V_B which is a three dimensional volume defined inside S^3 having the volume element in (A.4). Note that most of baryon charges are located inside the volume V_B of radius parameter λ_B as shown in (2.12). Explicitly $\langle r^2 \rangle_{M,p}^{1/2} = \sqrt{\frac{5}{6}} \lambda_B = 0.91 \lambda_B$, for instance.

Finally note also that the hypersphere coordinates (μ, θ, ϕ) are integrated out in (2.3), and E in (2.8) is a function of $\lambda_B = \frac{1}{ef_\pi}$ or equivalently f_π and e only. Moreover, the above physical quantities such as the moment of inertia, baryon masses and charge radii are also given by integral expressions similar to E in (2.3) and B in (2.5). These physical quantities are thus obtained in terms of f_π and e only, as shown in (2.10)–(2.12).

III. CHARGE DENSITY PROFILES IN HSM

In this section, we investigate the charge density profiles of nucleons in Fig. 1(b) and Fig. 1(c). Note that, as in the the profile function in the identity map in Fig. 1(a), these charge density profiles are formulated in terms of the angle μ . Moreover the charge density profiles $\rho_p(\mu)$ and $\rho_n(\mu)$ are associated with the charges inside the nucleons, while the profile function $f(\mu)$ in the identity map is related with the BPS bound in the soliton energy.

Now, using the hypersphere metric in (2.2), we construct the charge density profiles of proton and neutron

$$\rho_p(\mu) = \frac{1}{2} [\rho_{I=0}(\mu) + \rho_{I=1}(\mu)], \quad \rho_n(\mu) = \frac{1}{2} [\rho_{I=0}(\mu) - \rho_{I=1}(\mu)], \quad (3.1)$$

where the isoscalar and isovector electric charge densities are given by

$$\rho_{I=0}(\mu) = \frac{2}{\pi} \sin^2 \mu, \quad \rho_{I=1}(\mu) = \frac{8}{3\pi} \sin^4 \mu, \quad (3.2)$$

respectively, to produce

$$\rho_p(\mu) = \frac{1}{\pi} \sin^2 \mu \left(1 + \frac{4}{3} \sin^2 \mu \right), \quad \rho_n(\mu) = \frac{1}{\pi} \sin^2 \mu \left(1 - \frac{4}{3} \sin^2 \mu \right). \quad (3.3)$$

We then find the proton and neutron charges as follows

$$Q_p = \int_0^\pi d\mu \rho_p(\mu), \quad Q_n = \int_0^\pi d\mu \rho_n(\mu), \quad (3.4)$$

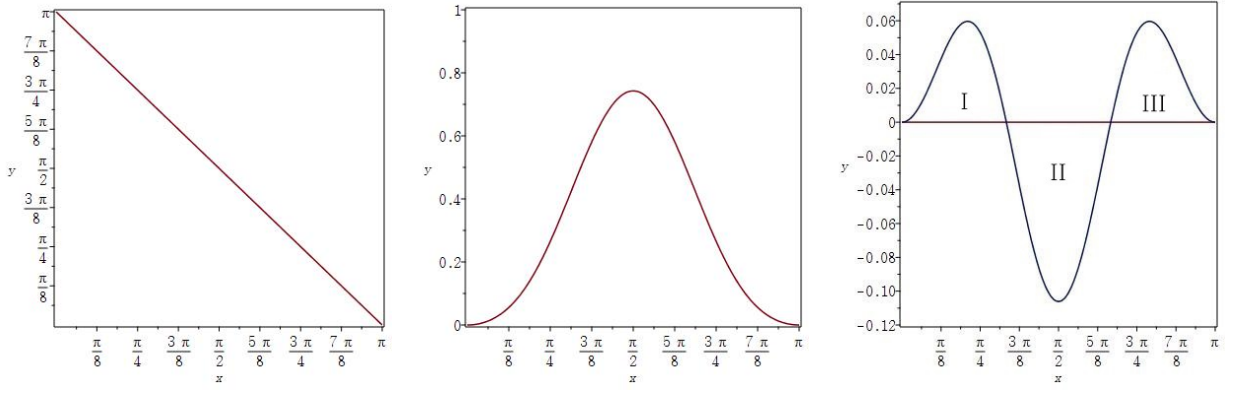


FIG. 1: (a) The profile function $f(\mu)$ in the identity map, and the charge density profiles (b) $\rho_p(\mu)$ and (c) $\rho_n(\mu)$, for proton and neutron respectively, are plotted versus μ . Here $f(\mu)$ is related with the BPS bound in the soliton energy, and $\rho_p(\mu)$ and $\rho_n(\mu)$ are associated with the charges inside the nucleons.

which yield $Q_p = 1$ and $Q_n = 0$ as expected.

The proton and neutron charge densities in (3.3) are depicted in Fig. 1(b) and Fig. 1(c), respectively. From (3.3) we find two root values of $\rho_n(\mu)=0$: $\mu = \frac{\pi}{3}$ and $\mu = \frac{2\pi}{3}$. We now have three regions I, II and III in the neutron charge density as shown in Fig. 1(c) and for each region, we obtain the charge fractions as follows

$$Q_n^I = \frac{\sqrt{3}}{16\pi}, \quad Q_n^{II} = -\frac{\sqrt{3}}{8\pi}, \quad Q_n^{III} = \frac{\sqrt{3}}{16\pi}, \quad (3.5)$$

which are in good agreement with the result $Q_n = 0$. Note that the charge density profiles of proton and neutron have no dependence on the coordinates θ and ϕ and they have dependence only on the coordinate μ on S^1 .

IV. TOPOLOGY AND KNOT STRUCTURE IN HSM

Now we investigate the topological aspects, knot structure, gluon effect and confinement in the hypersphere soliton. To this, we first consider the (1+1) dimensional sine-Gordon soliton whose Lagrangian is given in appropriate length and energy units as follows [18, 20–22]

$$L_{SG} = \int dx \left[\frac{1}{2} \partial_\mu \phi \partial^\mu \phi + \cos \phi - 1 \right], \quad (4.1)$$

from which we obtain the field equation of the form

$$\square \phi + \sin \phi = 0. \quad (4.2)$$

Note that the sine-Gordon field equation satisfies the discrete symmetry $\phi(x, t) \rightarrow \phi(x, t) + 2N\pi$, $N = 0, \pm 1, \pm 2, \dots$. The topological charge for a static solution of the sine-Gordon kink is then given by $Q_{top} = \frac{1}{2\pi} [\phi(+\infty) - \phi(-\infty)]$. We now have the static soliton solutions of the form: $\phi(x) = +4 \tan^{-1} \exp x$ and $\phi(x) = -4 \tan^{-1} \exp x$, for the cases of $Q_{top} = +1$ for a kink and $Q_{top} = -1$ for an anti-kink, respectively. These sine-Gordon kink solutions represent infinite Möbius strip feature [21]. Moreover the sine-Gordon kink state is identifiable as a fermion [22]. Note in the hypersphere soliton that, exploiting B in (2.5), we have the profile function $f(\mu) = \pi - \mu$ for the hypersphere soliton with the topological charge $B = +1$ [13, 18]. We also obtain $f(\mu) = -(\pi - \mu)$ for the hypersphere anti-soliton with $B = -1$ [18]. In this sense, in the hypersphere soliton, we can have the Möbius strip feature similar to that in the sine-Gordon kink.

Next we consider a *half-twist circle* S^1 inside S^3 which will be discussed in Appendix A,¹ in order to briefly investigate the relations between the three dimensional tubular neighborhood of the half-twist circle and the corresponding Möbius

¹ Here and in Appendix A, we use λ instead of λ_B for the radius parameter of hypersphere, for simplicity.

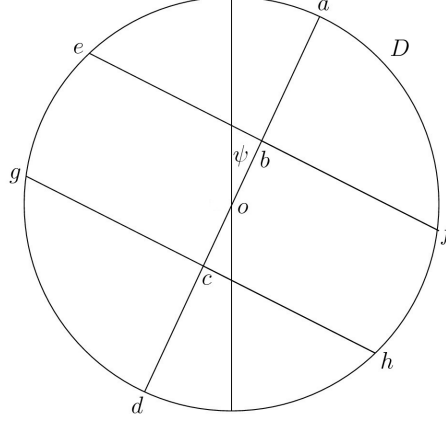


FIG. 2: The cross section of tubular neighborhood of the half-twist circle is delineated by the Möbius strip.



FIG. 3: (a) The Möbius strip corresponds to the fermion, and (b) the Möbius strip with knot structure explains the gluon effect and confinement problem.

strip. We now assume that the point o is the center of the two dimensional disc D representing the cross section of the tubular neighborhood of the half-twist circle as shown in Fig. 2. Here the line segment ad represents the cross section of the Möbius strip. Next we cut the disc D of the tubular neighborhood into three pieces by using the line segments ef and gh , and then we let the points b and c denote the corresponding cross sectional cutting lines on the Möbius strip. Here ψ represents the rotation angle of the disc D (or the line segment ad) with respect to the vertical line which is the initial position of D . As the disc D rotates along the circle S^1 of radius parameter λ , the angle ψ increases from 0 to π , to complete the cycle of the half-twist. In other words, after the complete rotation the final disc D arrives at the initial disc, with the angle shift π . By gluing these two discs together, we obtain a Möbius strip type tubular neighborhood of the half-twist circle S^1 . In particular the tubular neighborhood can be split into three pieces with nontrivial volume shapes along the half-twist circle. Moreover the line segment ad inside the tubular neighborhood makes the Möbius strip. In this respect without loss of generality, instead of the tubular neighborhoods of the half-twist circles S^1 inside S^3 , for visual clarity we will use the Möbius strips in Fig. 3(a) and Fig. 3(b) in the further discussions for the topology and knot structure of the baryons below.

Next note that, to describe a fermion such as a nucleon, we need a Möbius strip with a half-twist, associated with a half-twist circle in $S^3 = S^2 \times S^1$, as shown in Fig. 3(a). Here the half-twist circle S^1 plays a major role in the topological structure of the fermion. To relate the HSM to the quark model where, in the fermions such as proton and neutron, there exist three quarks, we separate the Möbius strip into three pieces as shown in Fig. 3(a) to yield two nontrivial Möbius strips which are linked to each other, as shown in Fig. 3(b). More specifically, we have the Möbius strip with the circumference length equal to that of the original Möbius strip in Fig. 3(a) and with a half-twist. This small Möbius strip originates from the middle piece of the Möbius strip in Fig. 3(a). Next we have the other Möbius strip with the circumference length of two times that of the original Möbius strip in Fig. 3(a) and with two twists. This large Möbius consists of the first and third pieces of the Möbius strip in Fig. 3(a). Note that the two twists of the large Möbius are equal to two times addition of two half-twists of the first and third pieces of the original Möbius strip. Moreover the large strip corresponds to uu in uud and dd in udd for proton and neutron defined in the quark

model, respectively. Now we emphasize that two Möbius strips in Fig. 3(b) are linked to produce a knot structure, which will be also discussed in Appendix A. Due to the knot structure, the soliton is unbroken to yield the strong interaction feature. In other words, the gluon effects in the quark model can be explained by the knot structure of the Möbius strips in the HSM.

It seems appropriate to comment on the confinement and asymptotic freedom [23–26]. In QCD, it is well known that strong interaction associated with the gluon effects is described in terms of confinement problem and asymptotic freedom. In the HSM there is no need to introduce the gluons, because the roles of the three quarks and the gluons, which bind the quarks, are replaced by those of the hypersphere soliton. Note that the hypersphere soliton is an extended object. As mentioned in Sec. II, most of charges fill the volume V_B of radius parameter λ_B , and the soliton itself is binded through its topological inner structure possessing the charge densities in Fig. 1(b) and Fig. 1(c). Moreover the confinement problem can be explained by the knot structure of the Möbius strips associated with the tubular neighborhoods of the half-twist circles inside the topological hypersphere soliton.

Finally we can classify the boson and fermion in terms of the strip structures. The boson performs 2π rotation to return its starting situation. This feature can be explained by exploiting 2π rotation on the ordinary strip. Next the fermion performs 4π rotation to return its initial situation according to the relativistic quantum mechanics. This feature can be explained by using 4π rotation on the Möbius strip shown in Fig. 3(a). The baryonic inner structure is thus successfully explained on the hypersphere S^3 . In contrast, in the case of bosonic inner structure, we do not need to consider such a hypersphere geometry.

V. CONCLUSIONS

In summary, we have constructed the physical quantities, such as masses and charge radii of the baryons, and have also obtained their profile functions and charge density profiles. To do this we have used the HSM where we have exploited the first class Hamiltonian, in order to predict the physical quantities more rigorously. Moreover, we have treated quantitative features of baryons by calculating the explicit isoscalar and isovector electric charge densities. In this approach we have formulated manifestly the proton and neutron charge densities and we have depicted the density distributions for proton and neutron plotted versus the hypersphere third angle μ . We have also investigated the topologies of the hypersphere soliton via the Möbius strips which are related with the tubular neighborhoods of the half-twist circles inside S^3 . In particular, we have shown that in the hypersphere soliton the baryons are delineated in terms of the knot structure of the Möbius strips. This knot structure of the Möbius strips can also explain the gluon effect and confinement problem of the quark related model such as QCD.

Acknowledgments

The author would like to thank Professor Peter van Nieuwenhuizen for helpful correspondence and kind encouragement. He was supported by Basic Science Research Program through the National Research Foundation of Korea funded by the Ministry of Education, NRF-2019R1I1A1A01058449.

Appendix A: Hypersphere geometry

In order to investigate a hypersphere of radius parameter λ , we consider the three metric on S^3

$$ds^2 = \lambda^2 d\mu^2 + \lambda^2 \sin^2 \mu (d\theta^2 + \sin^2 \theta d\phi^2). \quad (\text{A.1})$$

The ranges of the hyperspherical coordinates are given by $0 \leq \mu \leq \pi$, $0 \leq \theta \leq \pi$ and $0 \leq \phi \leq 2\pi$, and λ ($0 \leq \lambda < \infty$) is the radius parameter of S^3 . On the hypersphere, the three metric is given by the line element

$$d\vec{l} = \hat{e}_\mu \lambda d\mu + \hat{e}_\theta \lambda \sin \mu d\theta + \hat{e}_\phi \lambda \sin \mu \sin \theta d\phi, \quad (\text{A.2})$$

where $(\hat{e}_\mu, \hat{e}_\theta, \hat{e}_\phi)$ are the unit vectors along the three directions.

The area elements are given by

$$d\vec{a}_\mu = \hat{e}_\mu \lambda^2 \sin^2 \mu \sin \theta d\theta d\phi, \quad d\vec{a}_\theta = \hat{e}_\theta \lambda^2 \sin \mu \sin \theta d\mu d\phi, \quad d\vec{a}_\phi = \hat{e}_\phi \lambda^2 \sin \mu d\mu d\theta, \quad (\text{A.3})$$

and the three dimensional volume element is defined as

$$dV = \lambda^3 \sin^2 \mu \sin \theta d\mu d\theta d\phi. \quad (\text{A.4})$$

In the hyperspherical coordinates system, the gradient operator is given by

$$\nabla = \hat{e}_\mu \frac{1}{\lambda} \frac{\partial}{\partial \mu} + \hat{e}_\theta \frac{1}{\lambda \sin \mu} \frac{\partial}{\partial \theta} + \hat{e}_\phi \frac{1}{\lambda \sin \mu \sin \theta} \frac{\partial}{\partial \phi}. \quad (\text{A.5})$$

Next, we investigate a half-twist circle $S^1(\subset S^3)$ on the hypersphere. For the space manifolds S^3 and S^2 , we have the homotopy group [18, 27, 28] $\Pi_3(S^2) = \mathbf{Z}$. Note that in this homotopy group, the target space S^2 is a geometrical manifold. Due to the above homotopy group, we have an associated integer topological charge, namely the Hopf charge [18]. Here the Hopf charge is intrinsically different from the topological charge B associated with $\Pi_3(S^3) = \mathbf{Z}$. In other words, one cannot construct any Hopf charge having a form similar to B in (2.5). Instead, we have the preimage of a point on the target manifold S^2 which is a closed loop inside S^3 [18]. Moreover it is shown in the Hopf fibration [16–18] that the closed loop is a half-twist circle $S^1(\subset S^3)$. To be specific, noting that the homology groups for S^3 and $S^2 \times S^1$ are given by $H_1(S^3) = 0$ and $H_1(S^2 \times S^1) = \mathbf{Z}$ [29], one can find that the hypersphere S^3 is *locally* a product of two manifolds $S^3 = S^2 \times S^1$, implying that the $S^1(\subset S^3)$ is the half-twist circle of radius parameter λ . It is also interesting to note that the preimages inside S^3 decompose the hypersphere into a continuous family of circles, and two distinct circles are linked inside S^3 [17, 18] and form the Hopf link [30, 31].

-
- [1] P.A.M. Dirac, *Lectures on Quantum Mechanics* (Yeshiva University Press, New York, 1964).
 - [2] L. Castellani, P. van Nieuwenhuizen, M. Pilati, Phys. Rev. D **26**, 352 (1982).
 - [3] K. Schoutens, A. Sevrin, P. van Nieuwenhuizen, Commun. Math. Phys. **124**, 87 (1989).
 - [4] S.T. Hong, *BRST Symmetry and de Rham Cohomology* (Springer, Heidelberg, 2015), and references therein.
 - [5] C. Becchi, A. Rouet, R. Stora, Phys. Lett. B **52**, 344 (1974).
 - [6] C. Becchi, A. Rouet and R. Stora, Ann. Phys. **98**, 287 (1976).
 - [7] I.V. Tyutin, Levedev preprint, LEBEDEV-75-39 (1975).
 - [8] H. Nastase, M. Stephanov, P. van Nieuwenhuizen and A. Rebhan, Nucl. Phys. B **542**, 471 (1999), hep-th/9802074.
 - [9] D. Langlois, Class. Quantum Grav. **11**, 389 (1994).
 - [10] P. Malkiewicz, Class. Quantum Grav. **36**, 215003 (2019), arXiv:1810.11621.
 - [11] T.H.R. Skyrme, Proc. R. Soc. Lond. A **260**, 127 (1961).
 - [12] G.S. Adkins, C.R. Nappi, E. Witten, Nucl. Phys. B **228**, 552 (1983).
 - [13] S.T. Hong, Phys. Lett. B **417**, 211 (1998) [Corrigendum-ibid. **803**, 135179 (2020)].
 - [14] N.S. Manton, P.J. Ruback, Phys. Lett. B **181**, 137 (1986).
 - [15] S.T. Hong, Dirac quantization and baryon mass genesis in hypersphere soliton model, arXiv:2105.11456.
 - [16] H. Hopf, Math. Ann. **104**, 637 (1931).
 - [17] R. Bott, L.W. Tu, *Differential Forms in Algebraic Topology* (Springer, New York, 1982).
 - [18] N.S. Manton, P. Sutcliffe, *Topological Solitons* (Cambridge University Press, Cambridge, 2004).
 - [19] L.D. Faddeev, Lett. Math. Phys. **1**, 289 (1976).
 - [20] T.H.R. Skyrme, Proc. R. Soc. Lond. A **262**, 237 (1961).
 - [21] L.J. Boya, J. Mateos, *Group Theoretical Methods in Physics* (Springer-Verlag, Berlin, 1980), Editor: K.B. Wolf.
 - [22] R. Rajaraman, *Solitons and Instantons* (North-Holland, Amsterdam, 1987).
 - [23] D. Gross, F. Wilczek, Phys. Rev. Lett. **30**, 1343 (1973).
 - [24] H.D. Politzer, Phys. Rev. Lett. **30**, 1346 (1973).
 - [25] L.H. Ryder, *Quantum Field Theory* (Cambridge University Press, Cambridge, 1985).
 - [26] S. Pokorski, *Gauge Field Theories* (Cambridge University Press, Cambridge, 1987).
 - [27] H. Toda, *Composition Methods in Homotopy Groups of Spheres* (Princeton University Press, Princeton, 1962).
 - [28] A.S. Schwarz, *Quantum Field Theory and Topology* (Springer-Verlag, Berlin, 1993).
 - [29] J.J. Rotman, *An Introduction to Algebraic Topology* (Springer-Verlag, Heidelberg, 1988).
 - [30] L.H. Kauffman, *On Knots* (Princeton University Press, Princeton, 1987).
 - [31] J. Baez, J.P. Muniain, *Gauge Fields, Knots and Gravity* (World Scientific, Singapore, 1994).